Recent highlights in heavy flavour production and spectroscopy from LHCb

Patrick Spradlin

University of Glasgow | Experimental Particle Physics

UK Flavour 2017
04-06 September 2017
Institute for Particle Physics Phenomenology
Durham University, Durham, United Kingdom

Outline

1. Introduction

2. Production measurements
   - J/ψ cross-sections in pp at 13 TeV
   - B^+, B^0, B_s^0, Λ_b^0 production asymmetries in pp at 7 and 8 TeV
   - D^0 production in p-Pb at 5 TeV

3. Spectroscopy measurements
   - Introduction
   - Discovery of five new Ω_c^0 states
   - Amplitude analysis of $\Lambda_b^0 \to D^0 p \pi^-$
   - Ξ_b^- baryon spectroscopy
   - Discovery of Ξ_{cc}^{++}

Heavy flavor production at LHCb

A huge and expanding set of topics

Panoply of production environments,

- Inclusive production in *pp* collisions at 2.8, 5, 7, 8, and 13 TeV,
- Exclusive production in *pp* collisions at 7 and 13 TeV,
- Production in *p*-Pb collisions at $\sqrt{s_{\mathrm{NN}}} = 5$ and 8 TeV,
- Production in *p* collisions with gaseous fixed targets.

Abundance of observables,

- Differential cross-sections and production ratios,
- Particle Polarization,
- Particle-antiparticle asymmetries,
- Particle correlations.

Assortment of species,

- Hadrons with open heavy flavor,
- Charmonium and bottomonium states,
- Pairwise combinations for correlation measurements.

The program and its prospects: a daunting combinatoric problem.

HEAVY FLAVOR PRODUCTION PUBLICATIONS

Coll	$\sqrt{s_{NN}}$ (TeV)	State	Obs	LHCb PAPER	
pp	2.76	J/ψ	$d\sigma/dp_T$	2012-039	JHEP 1302 041
pp	2.76	$\Upsilon(nS)$	$d\sigma/dp_T \cdot \mathcal{B}$	2013-066	Eur.Phys.J. C74 2835
pp	5	D^0, $D^+_{(s)}$, D^{*+}	$d^2\sigma/dp_T dy$	2016-042	JHEP 1706 147
pp	7	J/ψ	$d^2\sigma/dp_T dy$	2011-003	Eur.Phys.J. C71 1645
pp	7	J/ψ	Pol	2013-008	Eur.Phys.J. C73 2631
pp	7	$\psi(2S)$	$d\sigma/dp_T$	2011-045	Eur.Phys.J. C72 2100
pp	7	$\psi(2S)$	Pol	2013-067	Eur.Phys.J. C74 2872
pp	7	$\Upsilon(nS)$	$d^2\sigma/dp_T dy \cdot \mathcal{B}$	2011-036	Eur.Phys.J. C72 2025
pp	7	χ_c, J/ψ	$\frac{\sigma(\chi_c)}{\sigma(\chi_c)}(p_T)$	2011-030	PLB 718 431-440
pp	7	$\chi_{c0}, \chi_{c1}, \chi_{c2}$	$\frac{\sigma(\chi_{c2})}{\sigma(\chi_{c1})}(p_T)$	2013-028	JHEP 1310 115
pp	7	χ_{c1}, χ_{c2}	$\frac{\sigma(\chi_{c2})}{\sigma(\chi_{c1})}(p_T)$	2011-019	PLB 714 215-223
pp	7	χ_b	$\mathcal{R}^{\chi_b}_{\Upsilon}$	2012-015	JHEP 1211 031
pp	7	$X(3872)$	$\sigma \cdot \mathcal{B}$	2011-034	Eur.Phys.J. C72 1972
pp	7	D^0, $D^+_{(s)}$, D^{*+}, Λ_c^+	$d^2\sigma/dp_T dy$	2013-009	Nucl.Phys. B871 1-20
pp	7	$D^\pm$	A_P	2012-305	PLB 718 902-909
pp	7	$D_s^\pm$	A_P	2012-009	PLB 713 186-195
pp	7	$b \to c\mu^-\overline{\nu}_\mu$	$d\sigma/d\eta$	2010-002	PLB 694 209-216
pp	7	$b \to c\mu^-\overline{\nu}_\mu$	$\frac{f_{s,\Lambda_b}}{f_u+f_d}$	2011-018	Phys.Rev. D85 032008
pp	7	$B^\pm$	$d\sigma/dp_T$	2011-043	JHEP 1204 093

HEAVY FLAVOR PRODUCTION PUBLICATIONS

pp	7	B^+, B^0, B^0_s	$\mathrm{d}^2\sigma/\mathrm{d}p_\mathrm{T}\mathrm{d}y$	2013-004	JHEP 1308 117
pp	7	B^0, B^0_s	$\frac{f_s}{f_d}$	2011-006	PRL 107 211801
pp	7	B^0_s, B^0	$\frac{f_s}{f_d}(p_\mathrm{T})$	2012-037	JHEP 1304 001
pp	7	B^0, B^0_s	A_P	2014-042	PLB 739 218-228
pp	7	B^+_c	$\frac{\sigma\cdot\mathcal{B}(B^+_c)}{\sigma\cdot\mathcal{B}(B^+)}$	2012-275	PRL 109 232001
pp	7	Λ^0_b	$\frac{f_{\Lambda_b}}{f_d}(p_\mathrm{T},\eta)$	2014-004	JHEP 1408 143
pp	7	Λ^0_b	Trans Pol	2013-020	PLB 724 27-35
pp	7	$J/\psi + J/\psi$	σ	2011-013	PLB 707 52-59
pp	7	$C_1 + C_2$ $\{J/\psi, D^0, D^+_{(s)}, \Lambda^+_c\}$	σ	2012-003	JHEP 1206 141 add. JHEP 1403 108
pp	7	$Z + (D^0, D^+)$	σ	2013-062	JHEP 1404 091
pp	7	$b\overline{b}$	Chg Asym	2014-023	PRL 113 no.8, 082003
pp	7 & 8	$\Upsilon(nS)$	$\mathrm{d}^2\sigma/\mathrm{d}p_\mathrm{T}\mathrm{d}y$	2015-045	JHEP 1511 103
pp	7 & 8	χ_b	$\mathcal{R}^{\chi_b}_{\Upsilon}$	2014-031	Eur.Phys.J. C74 3092
pp	7 & 8	χ_{b1}, χ_{b2}	$\frac{\sigma(\chi_{b2})}{\sigma(\chi_{b1})}$	2014-040	JHEP 1410 088
pp	7 & 8	η_c	$\mathrm{d}\sigma/\mathrm{d}p_\mathrm{T}$	2014-029	Eur.Phys.J. C75 311
pp	7 & 8	B^0, Λ^0_b	$\mathrm{d}^2\sigma/\mathrm{d}p_\mathrm{T}\mathrm{d}y$	2015-032	Chin.Phys. C40 011001
pp	7 & 8	$B^\pm$	A_P	2016-054	Phys.Rev. D95 052005
pp	7 & 8	B^+, $B^0_{(s)}$, Λ^0_b	$A_\mathrm{P}(p_\mathrm{T}, y)$	2016-062	arXiv:1703.08464
pp	7 & 8	$b\overline{b}$	Kin corr	2017-020	arXiv:1708.05994

HEAVY FLAVOR PRODUCTION PUBLICATIONS

pp	7 & 8	$\Upsilon + D$	$\mathrm{d}\sigma/\mathrm{d}p_{\mathrm{T}}$	2015-046	JHEP 1607 052
pp	8	J/ψ, $\Upsilon(nS)$	$\mathrm{d}^2\sigma/\mathrm{d}p_{\mathrm{T}}\mathrm{d}y$	2013-016	JHEP 1306 064
pp	8	B_c^+	$\frac{\sigma\cdot\mathcal{B}(B_c^+)}{\sigma\cdot\mathcal{B}(B^+)}(p_{\mathrm{T}}, y)$	2014-050	PRL 114 132001
pp	8	$W + q\overline{q}$	σ	2016-038	PLB 767 110-120
pp	13	J/ψ	$\mathrm{d}^2\sigma/\mathrm{d}p_{\mathrm{T}}\mathrm{d}y$	2015-037	JHEP 1510 172 err. JHEP 1705 063
pp	13	D^0, $D^+_{(s)}$, D^{*+}	$\mathrm{d}^2\sigma/\mathrm{d}p_{\mathrm{T}}\mathrm{d}y$	2015-041	JHEP 1603 159 err. JHEP 1609 013 err. JHEP 1705 074
pp	7 & 13	$b \to c\mu^-\overline{\nu}_\mu$	$\mathrm{d}^2\sigma/\mathrm{d}p_{\mathrm{T}}\mathrm{d}\eta$	2016-031	PRL 118 no.5, 052002
pp	13	$J/\psi + J/\psi$	$\mathrm{d}\sigma/\mathrm{d}p_{\mathrm{T}}$	2016-057	JHEP 1706 047
pp ex	7	J/ψ, $\psi(2S)$	σ	2012-044	J.Phys. G40 045001
pp ex	7	J/ψ, $\psi(2S)$	$\mathrm{d}\sigma/\mathrm{d}y$	2013-059	J.Phys. G41 055002
pp ex	7 & 8	$\Upsilon(1S)$, $\Upsilon(2S)$	$\mathrm{d}\sigma/\mathrm{d}y$	2015-011	JHEP 1509 084
pp ex	7 & 8	$J/\psi + J/\psi$	σ	2014-027	J.Phys. G41 115002
pp ex	13	J/ψ, $\psi(2S)$	$\mathrm{d}\sigma/\mathrm{d}y$	CONF-2016-007	
p-Pb	5	J/ψ	$\mathrm{d}^2\sigma/\mathrm{d}p_{\mathrm{T}}\mathrm{d}y$	2013-052	JHEP 1402 072
p-Pb	5	$\psi(2S)$	$\mathrm{d}\sigma/\mathrm{d}p_{\mathrm{T}}$, R_{FB}	2015-058	JHEP 1603 133
p-Pb	5	$\Upsilon(1S)$, $\Upsilon(2S)$	R_{FB}	2014-015	JHEP 1407 094
p-Pb	5	D^0	$\mathrm{d}^2\sigma/\mathrm{d}p_{\mathrm{T}}\mathrm{d}\eta$	2017-015	arXiv:1707.02750
p-Pb	8.16	J/ψ	$\mathrm{d}^2\sigma/\mathrm{d}p_{\mathrm{T}}\mathrm{d}\eta$	2017-014	arXiv:1706.07122
p-Ar	0.11	J/ψ, D^0	$\mathrm{d}N/\mathrm{d}p_{\mathrm{T}}$, *etc.*	CONF-2017-001	

THE LHCb DETECTOR

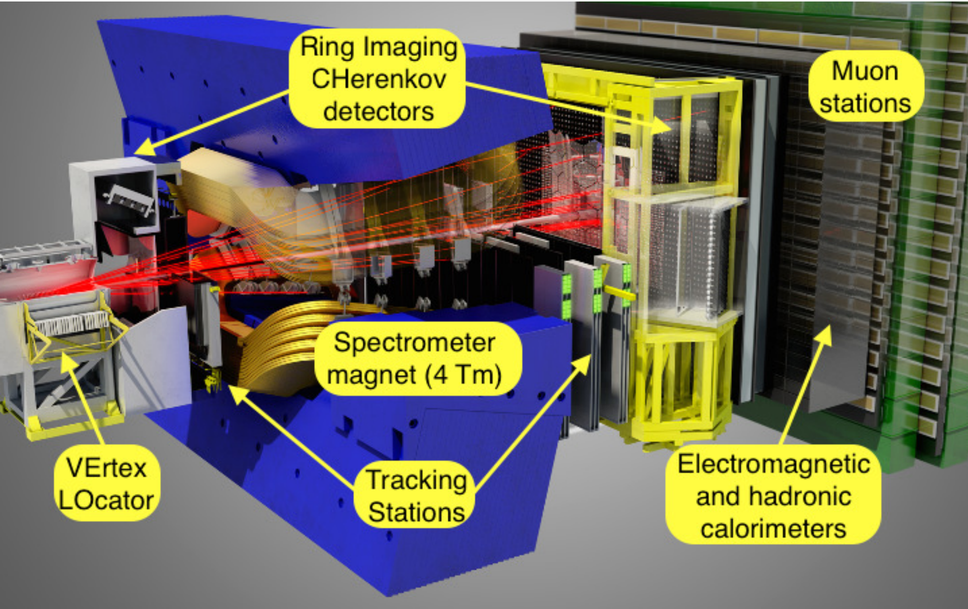

LHCb ACCEPTANCE

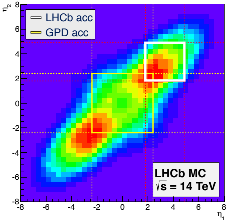

Pseudorapidity of b and $\overline{b}$ produced in pp collisions for LHCb simulation.

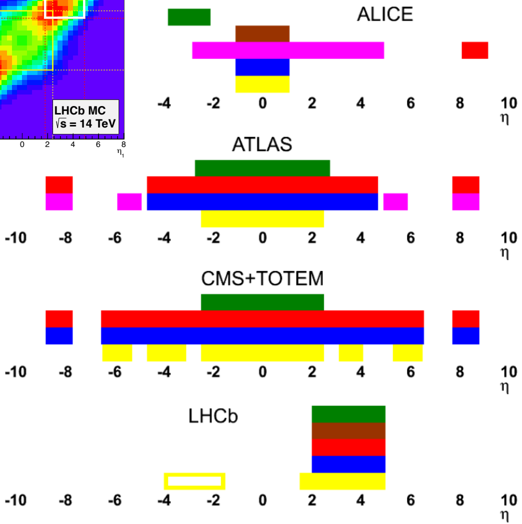

- ALICE
  - ➜ central
  - ➜ forward muon coverage
- ATLAS & CMS
  - ➜ central detectors
- LHCb
  - ➜ forward detector
  - ➜ tracking, particle-ID and calorimetry in full acceptance

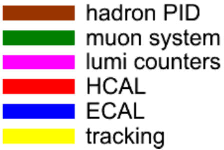

HEAVY PRODUCTION AND PROTON STRUCTURE

Heavy flavor forward production in LHC proton-proton collisions primarily through gluon-gluon fusion.

LHCb flavor production measurements cover a partonic momentum fraction x complementary to the HERA DIS data,

- HERA: $10^{-4} < x \lesssim 10^{-1}$,
- LHCb: $5 \times 10^{-6} < x \lesssim 10^{-4}$.

Inclusion of LHCb data should improve precision of gluon PDFs at small x,

- Implications for lepton flux calculations in atmospheric showers.

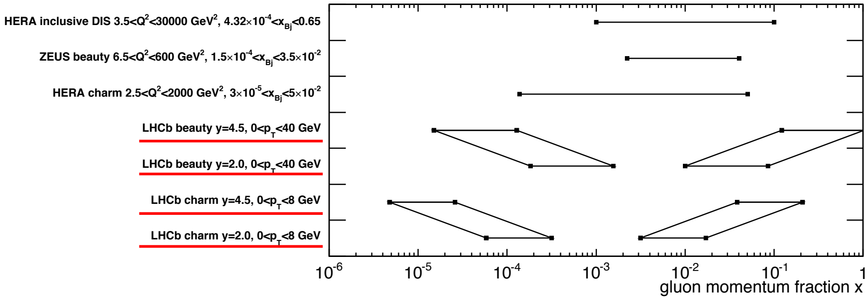

PROSA Collaboration, EPJ C75 (2015) 8, 396.

DIFFERENTIAL CROSS-SECTIONS

Differential production cross-sections of D mesons (H_c),

$$\frac{\mathrm{d}^2\sigma_i(H_c)}{\mathrm{d}p_\mathrm{T}\mathrm{d}y} = \frac{1}{\Delta p_\mathrm{T}\,\Delta y} \cdot \frac{N_i(H_c \to f + \text{c.c.})}{\varepsilon_{i,\mathrm{tot}}(H_c \to f) \cdot \mathcal{B}(H_c \to f) \cdot \mathcal{L}_\mathrm{int}}$$

in bins of p_T and y with respect to the collision axis.

- $N_i(H_c \to f + \text{c.c.})$: signal yield in bin i,
- $\varepsilon_{i,\mathrm{tot}}(H_c \to f)$: total signal efficiency
  - Factorized into components, *e.g.*, track reconstruction efficiency, PID efficiency, selection efficiency, *etc.*
  - Components evaluated in independent data samples where possible,
  - Estimated from simulation when not possible.
- $\mathcal{L}_\mathrm{int}$: integrated luminosity of sample,

Charm in hadronic collisions

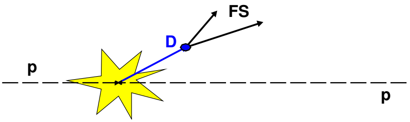

Prompt production

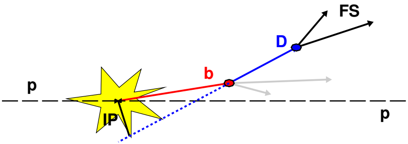

b decays ($B \to D^{(*)}X$)

Two major sources of charm:

- Prompt: Produced at primary interaction,
  - Direct production,
  - Feed-down from higher resonances.
- Secondary: Produced in the decay of a b-hadron.

Separate the prompt and secondary components,

- For J/ψ measurements, used to measure b-production cross-section,
- Secondary treated as background for D meson cross-sections.

J/ψ CROSS-SECTIONS

JHEP 1510 (2015) 172, ibid. 1705 (2017) 063

Integrated luminosity of $3.05 \pm 0.12\,\text{pb}^{-1}$

Analysis of trigger candidates with Turbo† stream.

† Comput. Phys. Commun. 208, 35-42

Separation of prompt J/ψ and J/ψ form b with pseudo-decay time

$$t_z = \frac{(z_{J/\psi} - z_{\text{PV}})M_{J/\psi}}{p_z}$$

Double differential cross-sections

$$\frac{\mathrm{d}^2\sigma_i(H_c)}{\mathrm{d}p_\mathrm{T}\mathrm{d}y}$$

for both prompt J/ψ and J/ψ from b.

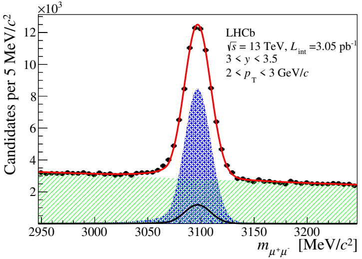

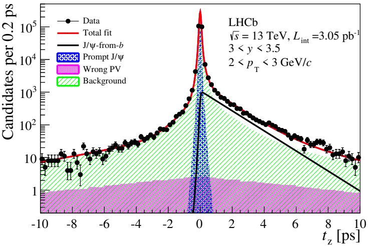

PROMPT J/ψ CROSS-SECTIONS

JHEP 1510 (2015) 172, ibid. 1705 (2017) 063

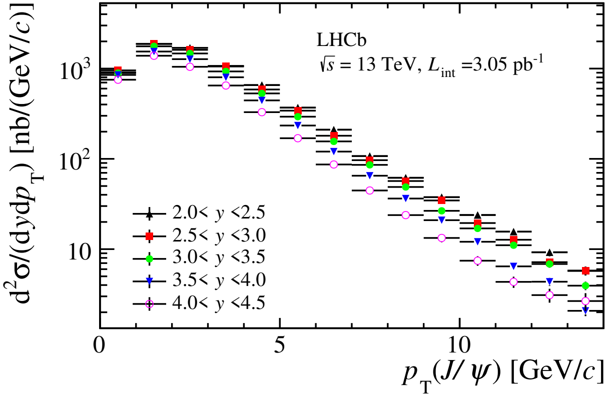

Double differential cross-sections, $\mathrm{d}^2\sigma_i/\mathrm{d}p_\mathrm{T}\mathrm{d}y$, of prompt J/ψ vs. p_T.

Integrated over the acceptance of the analysis

$$\sigma(\text{prompt } J/\psi\,, p_\mathrm{T} < 14\,\mathrm{GeV}, 2.0 < y < 4.5) = 15.03 \pm 0.03 \pm 0.94\,\mu\mathrm{b}.$$

PROMPT J/ψ CROSS-SECTIONS

JHEP 1510 (2015) 172, ibid. 1705 (2017) 063

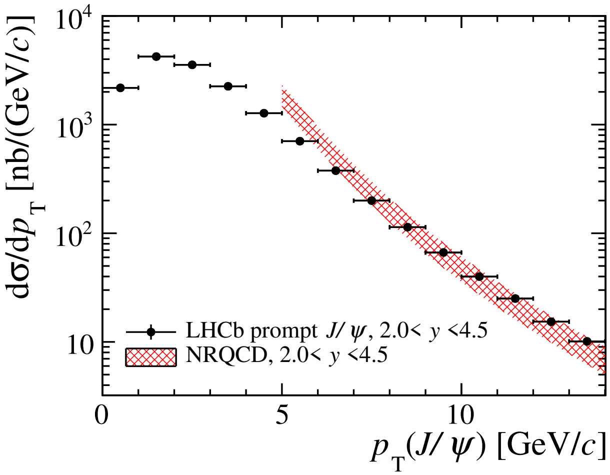

Differential cross-sections, $\mathrm{d}\sigma_i/\mathrm{d}p_\mathrm{T}$, integrated over $2.0 < y < 4.5$ and compared to NRQCD calculations (Shao *et al.*, JHEP 1505 (2015) 103).

J/ψ-FROM-b CROSS-SECTIONS

JHEP 1510 (2015) 172, ibid. 1705 (2017) 063

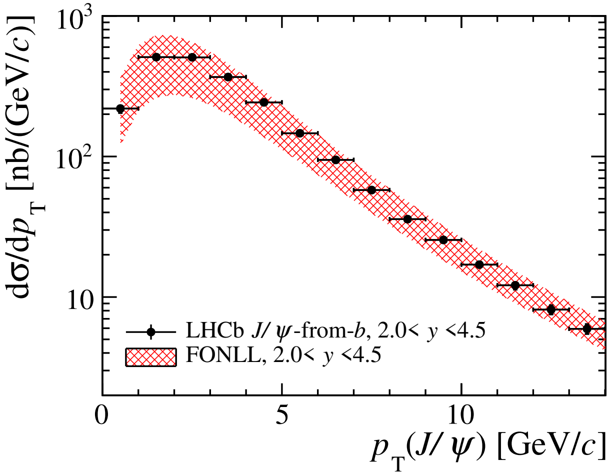

Differential cross-sections, $\mathrm{d}\sigma_i/\mathrm{d}p_{\mathrm{T}}$, integrated over $2.0 < y < 4.5$ and compared to FONLL calculations (Cacciari *et al.*, EPJ C75 (2015) 12, 610).

FORWARD J/ψ CROSS-SECTION AS A FUNCTION OF $\sqrt{s}$

JHEP 1510 (2015) 172, ibid. 1705 (2017) 063

Prompt J/ψ production cross-sections integrated over LHCb fiducial region:

$\sigma(\text{prompt } J/\psi, \text{LHCb}, 13\,\text{TeV}) = 15.03 \pm 0.03 \pm 0.94\ \mu\text{b}.$

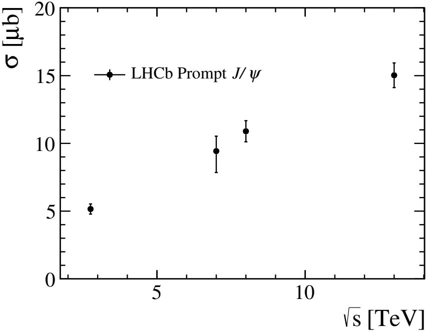

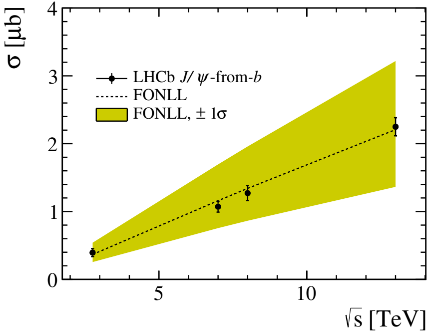

FONLL: Cacciari *et al.*, EPJ C75 (2015) no.12, 610

$\sigma(J/\psi\text{-from-}b, \text{LHCb}, 13\,\text{TeV}) = 2.25 \pm 0.01 \pm 0.14\ \mu\text{b}.$

Using a model based on PYTHIA6, extrapolate to a total 4π $b\bar{b}$ cross-section:

$\sigma(pp \to b\bar{b}X, 4\pi, 13\,\text{TeV}) = 495 \pm 2 \pm 52\ \mu\text{b}.$

COMPARISONS WITH 8 TeV

JHEP 1510 (2015) 172, ibid. 1705 (2017) 063

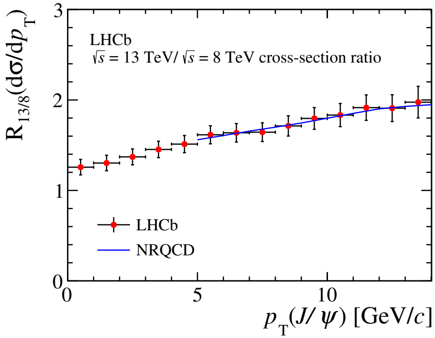

Ratios of differential cross-sections, $d\sigma_i/dp_T$, integrated over y between measurements at $\sqrt{s} = 13$ TeV and at $\sqrt{s} = 8$ TeV and compared to FONLL (Cacciari *et al.*, EPJ C75 (2015) 12, 610).

Ratios of differential cross-sections, $d\sigma_i/dp_T$, integrated over y between measurements at $\sqrt{s} = 13$ TeV and at $\sqrt{s} = 8$ TeV and compared to NRQCD (Shao *et al.*, JHEP 1505 (2015) 103).

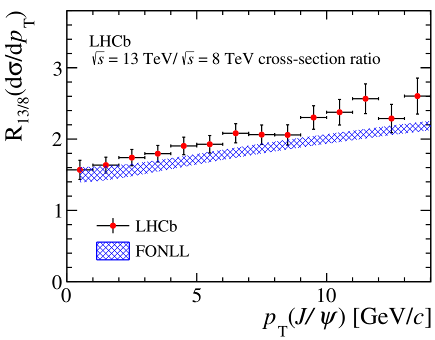

b-HADRON PRODUCTION ASYMMETRIES

arXiv:1703.08464, submitted to PLB

Pair production of $b\bar{b}$ dominant,

- Availability of p valence quarks may introduce asymmetries.

Important in precision CP violation studies.

Measured for B^0, B^+, and B_s^0 as functions of (p_{T}, y)

$$A_{\mathrm{P}} \equiv \frac{\sigma(\overline{H}_b) - \sigma(H_b)}{\sigma(\overline{H}_b) + \sigma(H_b)}$$

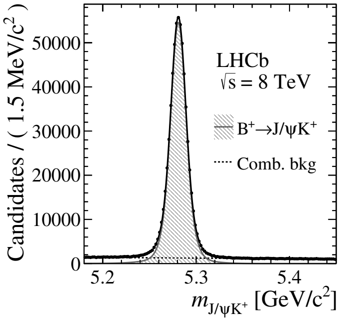

Determined for Λ_b^0 from

$$A_{\mathrm{P}}(\Lambda_b^0) = -\left[\frac{f_u}{f_{\Lambda_b^0}} A_{\mathrm{P}}(B^+) + \frac{f_d}{f_{\Lambda_b^0}} A_{\mathrm{P}}(B^0) + \frac{f_s}{f_{\Lambda_b^0}} A_{\mathrm{P}}(B_s^0) + \mathcal{O}(2 \cdot 10^{-3})\right].$$

fragmentation fractions from JHEP 1304 001, JHEP 1408 143.

Previous LHCb measurements: B^0, B_s^0: Phys. Lett. B739 218; Λ_b^0: Chin. Phys. C 40 011001.

ASYMMETRY MEASUREMENTS

arXiv:1703.08464, submitted to PLB

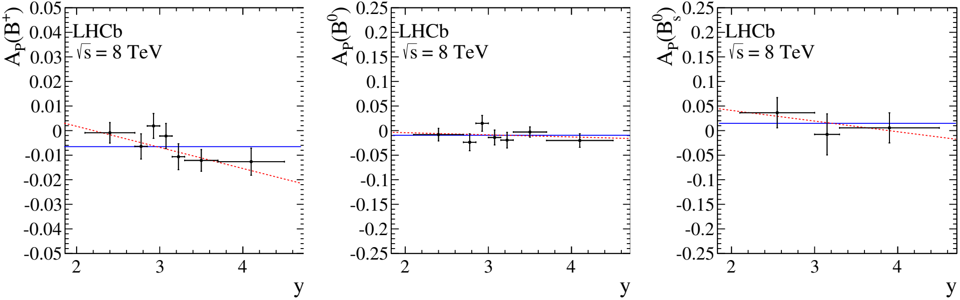

Integrated over fiducial range of measurements

	A_P $\sqrt{s} = 7$ TeV	A_P $\sqrt{s} = 8$ TeV
B^+	$-0.0023 \pm 0.0024 \pm 0.0037$	$-0.0074 \pm 0.0015 \pm 0.0032$
B^0	$0.0044 \pm 0.0088 \pm 0.0011$	$-0.0140 \pm 0.0055 \pm 0.0010$
B_s^0	$-0.0065 \pm 0.0288 \pm 0.0059$	$0.0198 \pm 0.0190 \pm 0.0059$
Λ_b^0	$-0.0011 \pm 0.0253 \pm 0.0108$	$0.0344 \pm 0.0161 \pm 0.0076$

D^0 PRODUCTION IN p-Pb COLLISIONS

Heavy flavor production can be used to study the properties of quark-gluon plasma in nucleus-nucleus collisions

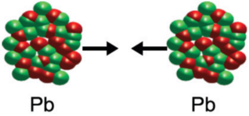

However, the cold nuclear matter effects must be disentangled from plasma effects. These can be studied in nucleon-nucleus (p-Pb) collisions

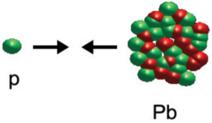

The study of cold nuclear matter effects relies on nucleon-nucleon interactions (p-p) as a reference.

LHCb collected p-Pb data at mean nucleon-nucleon collision energy $\sqrt{s_{\rm NN}} = 5\,\text{TeV}$.

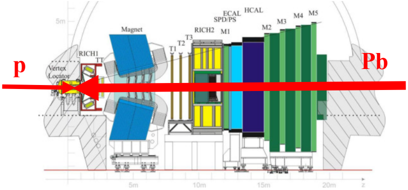

p on Pb collisions (forward)
$\mathcal{L}_{\rm int} \sim 1.1\,{\rm nb}^{-1}, \quad 1.5 < y^*(D) < 4.0.$

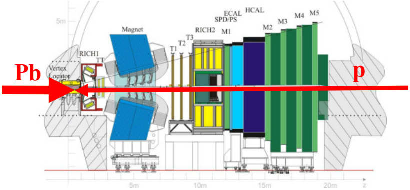

Pb on p collisions (backward)
$\mathcal{L}_{\rm int} \sim 0.5\,{\rm nb}^{-1}, \quad -5.0 < y^*(D) < -2.5.$

D^0 CROSS-SECTIONS IN p-Pb

arXiv:1707.02750, submitted to JHEP

Double-differential D^0 production cross-sections in p-Pb, $d^2\sigma/dy^* dp_T$,

- y^* and p_T in the nucleon-nucleon CoM,
- Measured wrt. the p momentum direction.

Forward-backward cross-section asymmetry:

$$R_{FB}(y^*, p_T; \sqrt{s_{NN}}) \equiv \frac{\sigma_{pPb}(+|y^*|, p_T; \sqrt{s_{NN}})}{\sigma_{pPb}(-|y^*|, p_T; \sqrt{s_{NN}})}.$$

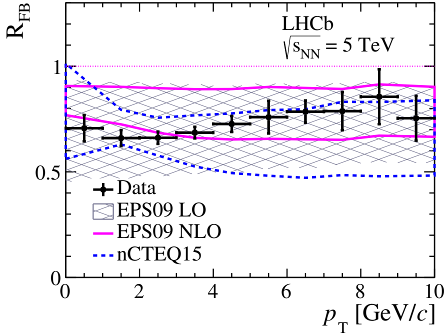

Forward ($p \to$ Pb)

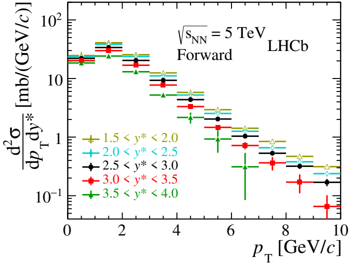

Backward (Pb$\to p$)

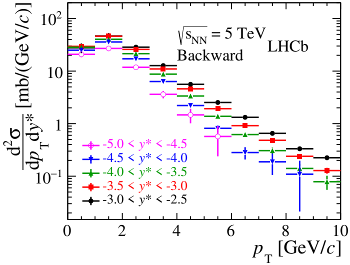

NUCLEAR MODIFICATION FACTOR

arXiv:1707.02750, submitted to JHEP

Effects of cold nuclear medium expressed relative *p-p* cross-sections:

$$R_{p\mathrm{Pb}}(y^*, p_\mathrm{T}; \sqrt{s_\mathrm{NN}}) \equiv \frac{1}{A}\frac{\mathrm{d}^2\sigma_{p\mathrm{Pb}}(y^*, p_\mathrm{T}; \sqrt{s_\mathrm{NN}})/\mathrm{d}y^*\mathrm{d}p_\mathrm{T}}{\mathrm{d}^2\sigma_{pp}(y^*, p_\mathrm{T}; \sqrt{s_\mathrm{NN}})/\mathrm{d}y^*\mathrm{d}p_\mathrm{T}}, A = 208$$

This preliminary result determined before the 5 TeV *p-p* cross-section,

- σ_{pp} estimated by extrapolation from the 7 TeV and 13 TeV cross-sections,
- Update in progress.

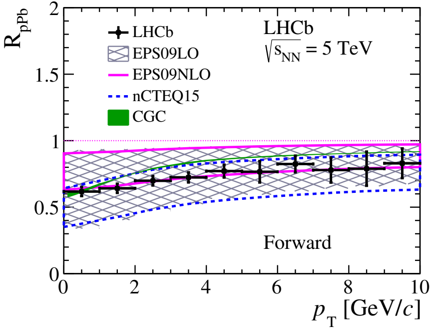

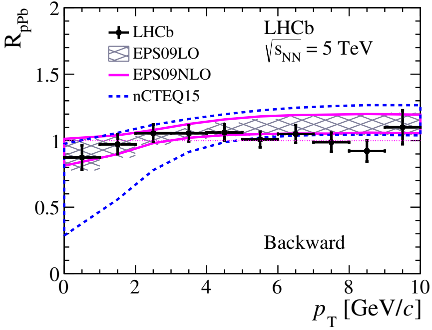

Spectroscopy measurements at LHCb

Inclusive studies of $H_{c,b} + h$

e.g., $pp \to (\Xi_c^+ K^-)_{\Omega^*} X$; $pp \to (\Xi_b^0 \pi^-)_{\Xi_b^{*-}} X$

- Applicable to all valence quark contents,
- All resonances are accessible,
- Large backgrounds,
- Spin-parity analysis only applicable to three-body decays,
  - Only distinguishes between natural and unnatural parity.

Amplitude analysis of multibody decays

- Applicable mainly to *c*-hadrons from *b*-hadron decays,
- Full spin-parity analysis,
- Limited access to high-mass resonances,
- Complicated analysis of multiple interfering states.

SEARCH FOR NEW Ω_c^0 STATES

Phys. Rev. Lett. 118, 182001

Previously, only two *css* baryons known: Ω_c^0 and $\Omega_c(2770)^0$.

Search for new Ω_c^0 states in the $\Xi_c^+ K^-$ mass spectrum.

Ξ_c^+ reconstructed in mode
$\Xi_c^+ \to pK^-\pi^+$,

- A Cabibbo-suppressed mode of Ξ_c^+, but very efficient.

Collated data from Runs 1 and 2

- 7 TeV: 1 fb^{-1},
- 8 TeV: 2 fb^{-1},
- 13 TeV: 0.3 fb^{-1}.

Total: $\sim 0.9 \times 10^6$ Ξ_c^+ decays.

Five new states decaying to $\Xi_c^+ K^-$

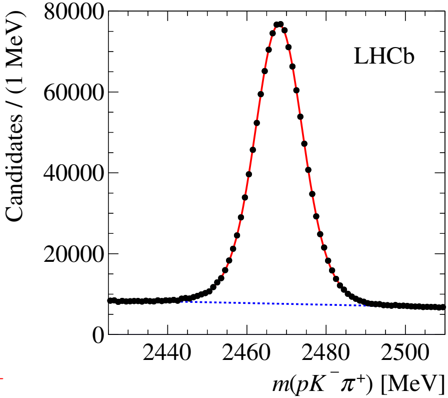

SPECTRUM OF $\Xi_c^+ K^-$

Phys. Rev. Lett. 118, 182001

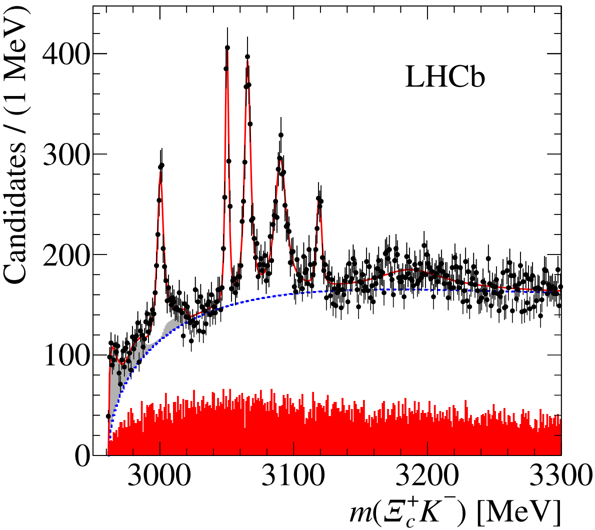

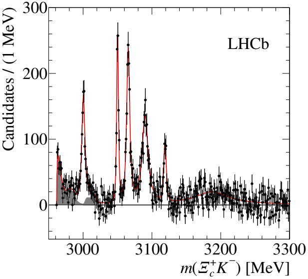

Background subtracted distributions.

MASSES AND WIDTHS OF NEW STATES

Phys. Rev. Lett. 118, 182001

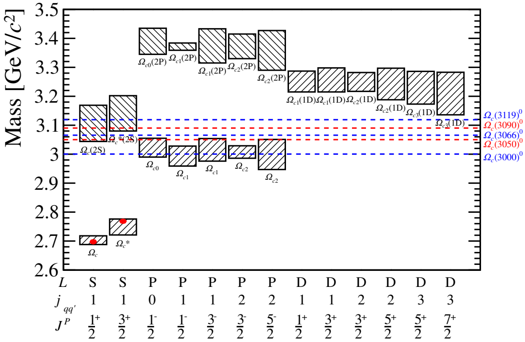

Resonance	Mass (MeV)	Γ (MeV)	Yield	N_σ
$\Omega_c(3000)^0$	$3000.4 \pm 0.2 \pm 0.1^{+0.3}_{-0.5}$	$4.5 \pm 0.6 \pm 0.3$	$1300 \pm 100 \pm 80$	20.4
$\Omega_c(3050)^0$	$3050.2 \pm 0.1 \pm 0.1^{+0.3}_{-0.5}$	$0.8 \pm 0.2 \pm 0.1$	$970 \pm 60 \pm 20$	20.4
		< 1.2 MeV, 95% CL		
$\Omega_c(3066)^0$	$3065.6 \pm 0.1 \pm 0.3^{+0.3}_{-0.5}$	$3.5 \pm 0.4 \pm 0.2$	$1740 \pm 100 \pm 50$	23.9
$\Omega_c(3090)^0$	$3090.2 \pm 0.3 \pm 0.5^{+0.3}_{-0.5}$	$8.7 \pm 1.0 \pm 0.8$	$2000 \pm 140 \pm 130$	21.1
$\Omega_c(3119)^0$	$3119.1 \pm 0.3 \pm 0.9^{+0.3}_{-0.5}$	$1.1 \pm 0.8 \pm 0.4$	$480 \pm 70 \pm 30$	10.4
		< 2.6 MeV, 95% CL		

AMPLITUDE ANALYSIS OF $\Lambda_b^0 \to D^0 p \pi^-$

arXiv:1708.05808, submitted to PRL

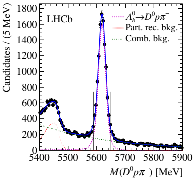

Amplitude analysis of 10,233 $\Lambda_b^0 \to D^0 p \pi^-$ decays

- Signal purity $\sim$86%.

Five-dimensional representation of the phase space.

Detailed study of $D^0 p$ amplitude, including Λ_c^+ resonance

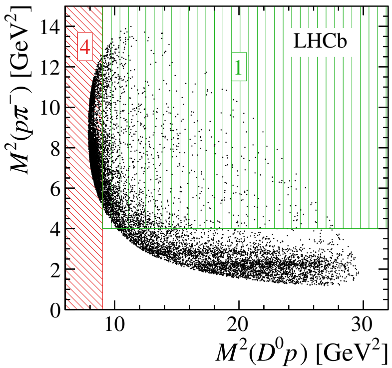

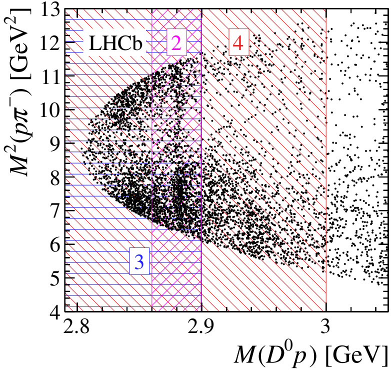

AMPLITUDE ANALYSIS OF $\Lambda_b^0 \to D^0 p\pi^-$

arXiv:1708.05808, submitted to PRL

Measured parameters:

$\Lambda_c(2880)^+$ preferred spin $J = \frac{5}{2}$

$m(\Lambda_c(2880)^+) = 2881.75 \pm 0.29 \pm 0.07^{+0.14}_{-0.20}$

$\Gamma(\Lambda_c(2880)^+) = 5.43^{+0.77}_{-0.71} \pm 0.29^{+0.75}_{-0.00}$

$\Lambda_c(2940)^+$ preferred $J^P = \frac{3}{2}^-$, but $\frac{1}{2}$ and $\frac{7}{2}$ not ruled out.

First analysis constraining J^P for this state.

$m(\Lambda_c(2940)^+) = 2944.8^{+3.5}_{-2.5} \pm 0.4^{+0.1}_{-4.6}$

$\Gamma(\Lambda_c(2940)^+) = 27.7^{+8.2}_{-6.0} \pm 0.9^{+5.2}_{-10.4}$

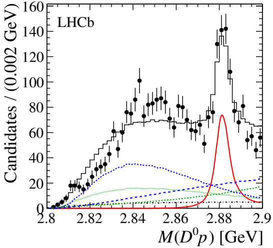

Fit with non-resonant and $\Lambda_c(2880)^+$

Threshold enhancement is consistent with a new resonance,

Designated $\Lambda_c(2860)^+$

Preferred $J^P = \frac{3}{2}^+$

$m = 2856.1^{+2.0}_{-1.7} \pm 0.5^{+1.1}_{-4.6}$

$\Gamma = 67.6^{+10.1}_{-8.1} \pm 1.4^{+5.9}_{-20.0}$

Fourth uncertainty is systematic due to model of non-resonant components.

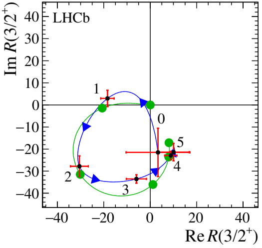

Argand diagram of partial wave analysis

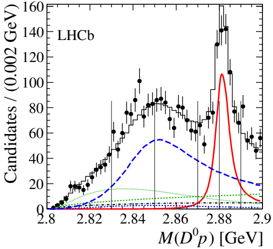

As above, with $\Lambda_c(2860)^+$

Ξ_b^- SPECTROSCOPY AT LHCb

PRL 114 (2015) 062004

Search for new Ξ_b^- states in the $\Xi_b^0\pi^-$ mass spectrum.

Ξ_b^0 reconstructed in mode $\Xi_b^0 \to \Xi_c^+\pi^-$, $\Xi_c^+ \to pK^-\pi^+$,

- $\Xi_c^+ \to pK^-\pi^+$ is a suppressed decay, but very efficiently detected.

Two new resonances observed.

Mass and width of the state measured.

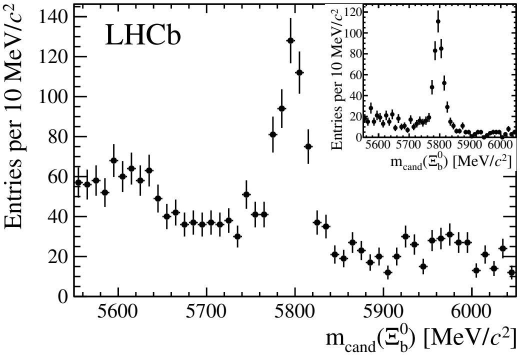

Inset: $m(\Xi_b^0)$ for $\Xi_b^0\pi^-$ candidates in $3.0 < \delta m < 4.2$ MeV and $21 < \delta m < 27$ MeV.

Relative production cross-section determined with respect to that of Ξ_b^0:

$$\frac{\sigma\left(pp \to \Xi_b^{\prime(*)-} X\right) \mathcal{B}\left(\Xi_b^{\prime(*)-} \to \Xi_b^0\pi^-\right)}{\sigma\left(pp \to \Xi_b^0 X\right)}$$

MASSES OF NEW STATES

PRL 114 (2015) 062004

Fits to *P*-wave relativistic Breit-Wigner line shapes convolved with a resolution function.

$\delta m(\Xi_b'^-) = 3.653 \pm 0.018 \pm 0.006\,\text{MeV}$	$\delta m(\Xi_b^{*-}) = 23.96 \pm 0.12 \pm 0.06\,\text{MeV}$
$\Gamma(\Xi_b'^-) < 0.08\,\text{MeV}$ at 95% C.L.	$\Gamma(\Xi_b^{*-}) = 1.65 \pm 0.31 \pm 0.10\,\text{MeV}$
$m(\Xi_b'^-) = 5935.02 \pm 0.02 \pm 0.01 \pm 0.50\,\text{MeV}$	$m(\Xi_b^{*-}) = 5955.33 \pm 0.12 \pm 0.06 \pm 0.50\,\text{MeV}$

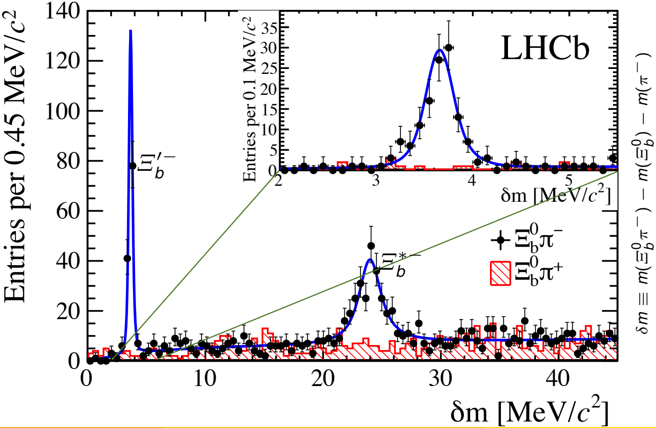

SEARCH FOR Ξ_b^0 OSCILLATIONS

arXiv:1708.05808

Exploit the newly discovered Ξ_b^- states to search for baryon-number violating Ξ_b^0 oscillations.

Initial state of Ξ_b^0 tagged by slow pion charge,

- Same-side tagging long used in D^0 mixing measurements.

Final state identified by decay products/final proton charge

$$\text{OS} \quad \Xi_b^{\prime,*-} \to (\Xi_c^+\pi^-)_{\Xi_b}\pi^-$$
$$\text{SS} \quad \Xi_b^{\prime,*-} \to (\overline{\Xi}_c^-\pi^+)_{\Xi_b}\pi^-$$

No mixing observed

- Mixing frequency $\omega < 0.08\,\text{ps}^{-1}$ at 95% C.L.

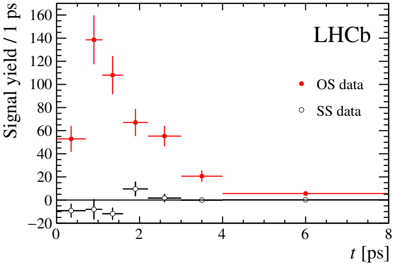

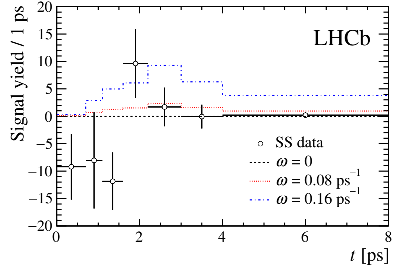

DOUBLY CHARMED BARYONS

The constituent-quark model predicts three weakly decaying $C = 2$, $J^P = \frac{1}{2}^+$ states: Ξ_{cc}^{+} (ccd), Ξ_{cc}^{++} (ccu), and Ω_{cc}^{+} (ccs).

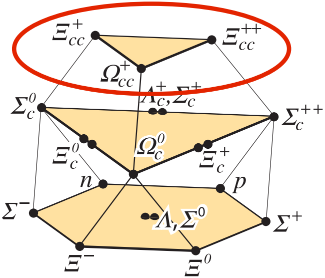

SU(4) flavor multiplets, PDG Review of Particle Physics, Phys.Rev. D86, 010001.

There are several theoretical predictions of their properties on the market:

- Masses: 3500-3700 MeV, (broad range of predictions)
- Lifetimes: $\tau(\Xi_{cc}^{+}) \approx \tau(\Omega_{cc}^{+}) < \tau(\Xi_{cc}^{++})$
  - $\tau(\Xi_{cc}^{+}) \approx$ 50 to 250 fs
  - $\tau(\Xi_{cc}^{++}) \approx$ 200 to 700 fs

SELEX AND Ξ_{cc}^{+}

Phys.Rev.Lett. 89 (2002) 112001, Phys.Lett. B628 (2005) 18-24

In 2002, SELEX, a fixed-target charm hadroproduction experiment at Fermilab, claimed the first observation of Ξ_{cc}^{+} in decays to $\Lambda_c^+ K^- \pi^+$.

Followed by a confirmation in 2004 in $D^+ p K^-$,

- $\Lambda_c^+ K^- \pi^+$: 15.9 sig over 6.1 bkg (6.3σ),
- $D^+ p K^-$: 5.62 sig over 1.38 bkg (4.8σ).

Combined mass:
$m(\Xi_{cc}^{+}) = 3518.7 \pm 1.7\,\mathrm{MeV}/c^2$.

Unexpected properties of the observation:

- Short lifetime, $\tau < 33\,\mathrm{fs}$ at 90% C.L.
- 20% of all Λ_c^+ production with baryon beams.

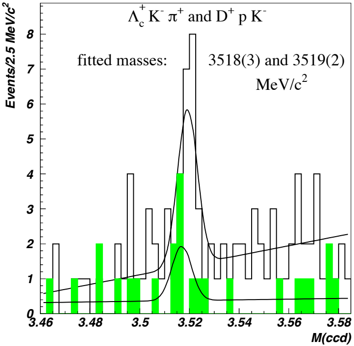

SELEX $\Lambda_c^+ K^- \pi^+$ and $D^+ p K^-$ distributions superposed
Phys.Lett. B628 (2005) 18-24

Unique production environment:

- Hyperon beam: admixture of Σ^- (68%), proton (18%), and π^- (13%),
- Thin foil target: Cu or diamond.

Reconstruction of $\Xi_{cc}^{++} \to \Lambda_c^+ K^- \pi^+ \pi^+$

arXiv:1707.01621, accepted by Phys.Rev.Lett.

Λ_c^+ combined with K^- and $2 \times \pi^+$ candidates,

- Unphysical 'wrong-sign' (WS) mode $\Lambda_c^+ K^- \pi^+ \pi^-$ also reconstructed.

Neural-network selector trained on simulated signal and wrong-charge data.

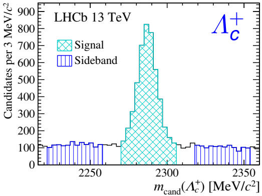

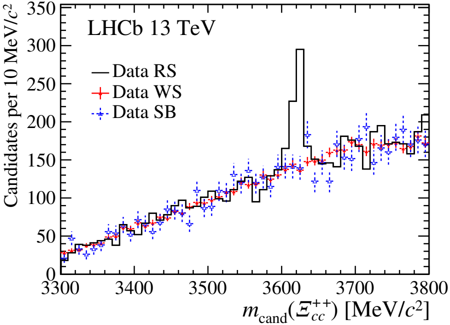

Clear structure visible at ~ 3620 MeV!

- No corresponding structure in WS nor in Λ_c^+ sidebands.

Likelihood fit in the range 3620 ± 150

- Yield: 313 ± 33 decays,
- Local significance: $> 12\sigma$ (likelihood ratio).

$$m(\Xi_{cc}^{++}) \equiv m[(pK^-\pi^+)_{\Lambda_c^+} K^-\pi^+\pi^+] - m[(pK^-\pi^+)_{\Lambda_c^+}] + m(\Lambda_c^+)_{\rm PDG}$$

MASS OF $\Xi_{cc}^{++} \to \Lambda_c^+ K^- \pi^+ \pi^+$

arXiv:1707.01621, accepted by Phys.Rev.Lett.

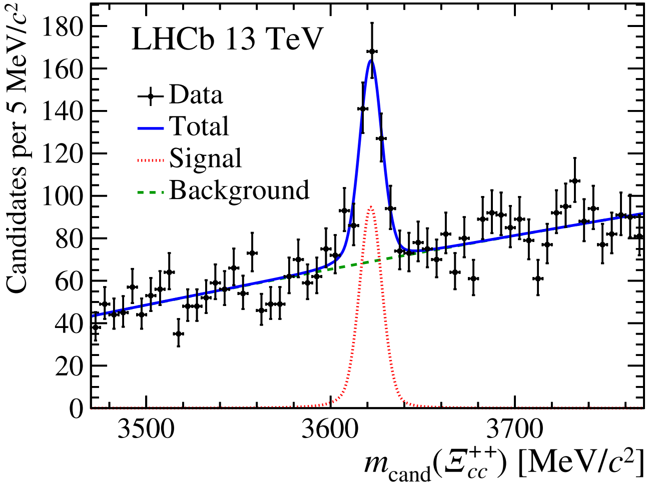

$m(\Xi_{cc}^{++}) = 3621.40 \pm 0.72\,(\text{stat}) \pm 0.27\,(\text{syst}) \pm 0.14(\Lambda_c^+)$ MeV

Weak decay

arXiv:1707.01621, accepted by Phys.Rev.Lett.

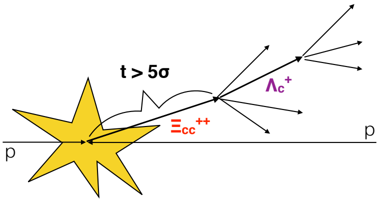

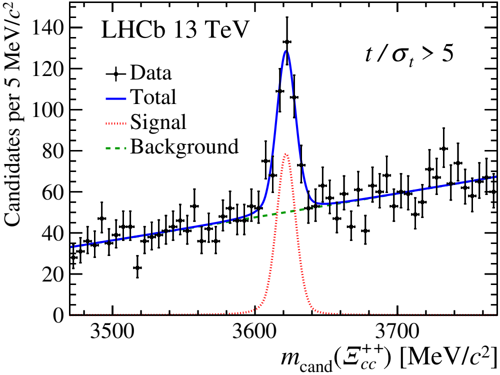

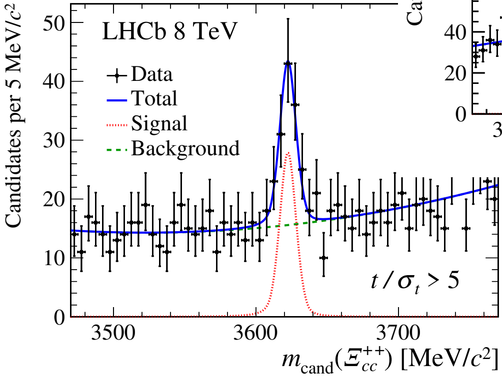

Decay time $> 5\sigma$ wrt the primary interaction vertex

- Run 1 significance: 7σ,
- Run 2 significance: 12σ.

Inconsistent with strong decay.

Comparison with SELEX

arXiv:1707.01621, accepted by Phys.Rev.Lett.

$$m(\Xi_{cc}^{++})_{\text{LHCb}} - m(\Xi_{cc}^{+})_{\text{SELEX}} = 103 \pm 2\,\text{MeV}$$

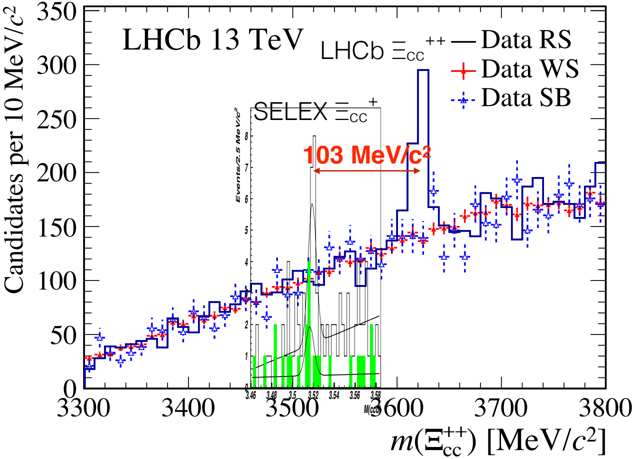

Inconsistent with being isospin partners.

[E.g., Hwang and Chung, PRD 78 073013; Brodsky, Guo, Hanhart, and Meissner, PLB 698 251-255; Karliner and Rosner, arXiv:1706.06961]

SUMMARY

LHCb's forward design allows it to probe a unique region of heavy flavor production at LHC.

Heavy flavor production measurements with broad applications

- Tests of QCD calculations methods,
- Refinements of proton PDFs,
  - ⇒ Improved understanding of backgrounds for cosmic neutrino studies.
- Cold nuclear matter effects for quark gluon plasma studies,
- Examinations of double parton scattering.

Discovery and characterization of new states,

- Inclusive studies based on huge charm samples,
- Amplitude analyses of large samples of $b \to c$ decays.

Backup

HEAVY FLAVOR PRODUCTION

Production measurements of heavy flavor hadrons can be vital to improved understanding of QCD,

- Test precise cross-section predictions,
- Provide empirical fragmentation functions,
- Probe proton structure at low x.

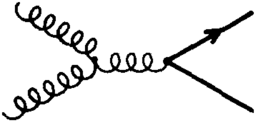

Necessary for MC generator tuning,

- Simulation inputs to precision flavor physics measurements,
- Long term program planning,
- New experiment design.

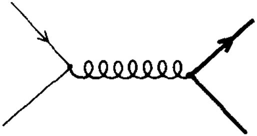

Standard Model backgrounds for New Physics searches,

- Absolute rates of SM processes must be known precisely.

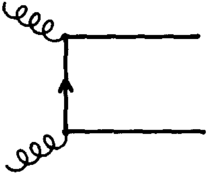

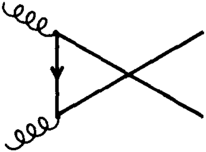

CHARM AND ASTROPHYSICAL NEUTRINOS

Atmospheric charm production and decay is a dominant source of background for ultra-high-energy neutrino astrophysics.

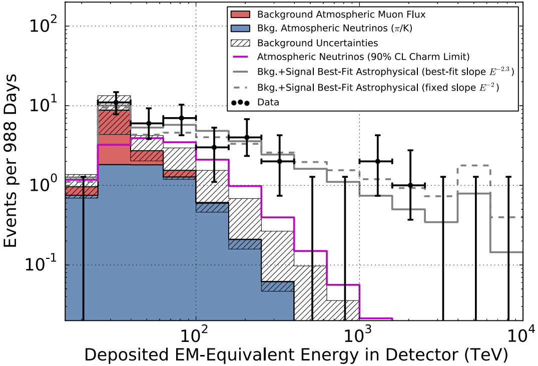

IceCube, PRL 113 (2014) 101101.

Energy of IceCube observed events with predictions of atmospheric sources and overall fit.

Neutrinos from atmospheric charm

LHC measurements relevant to neutrinos from atmospheric charm production,

- pp at $\sqrt{s} = 7\,\text{TeV}$ ($13\,\text{TeV}$) corresponds to incoming cosmic ray of $E = 26\,\text{PeV}$ ($90\,\text{PeV}$).

Gauld *et al.* performed a PDF improvement similar to PROSA,

- NNPDF3.0 NLO set reweighted to match LHCb charm cross-sections at $7\,\text{TeV}$.

Significant improvement in precision at small x.

Improved PDF set used in POWHEG and other MC generators,

- Charm production cross-sections in LHC $\sqrt{s} = 13\,\text{TeV}$ collisions,
- Atmospheric charm production in high-energy cosmic ray interactions.

See also Bhattacharya *et al.*, JHEP 06 (2015) 110.

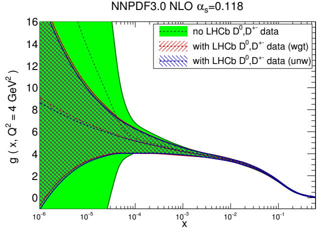

NNPDF3.0 NLO small-x gluon with LHCb charm

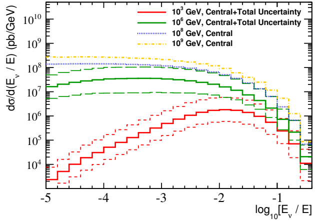

Differential cross-section of charm-induced neutrino production.

Gauld *et al.*, JHEP 1511 (2015) 009

INTRINSIC CHARM IN PROTONS

Intrinsic charm/beauty are hypothetical $c\bar{c}$ or $b\bar{b}$ contributions to the proton beyond the 'sea'.

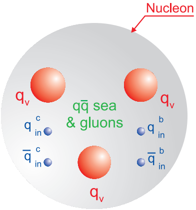

Several potential models have been explored in theory, including five-quark $uudc\bar{c}$ states and $D^0(u\bar{c})\Lambda_c^+(udc)$ quasi-two-body bound states.

cf. pentaquarks, Phys.Rev.Lett. 115 (2015) 072001.

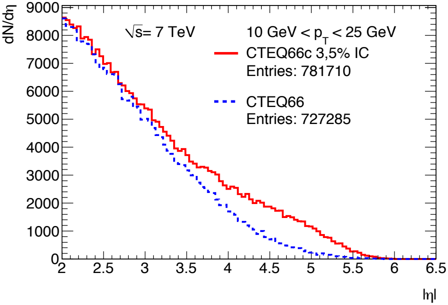

Europhys.Lett. 99 (2012) 21002 Fig. 9. Predicted $pp \to (D^0 + \bar{D}^0)X$ at $\sqrt{s} = 7\,\text{TeV}$ and $10 \leq p_{\text{T}} \leq 25\,\text{GeV}/c$.

Evidence for intrinsic heavy flavor can manifest in production spectra.

Enhances forward production,

- Up to a factor of 3–10 for forward Λ_b^0 or Λ_c^+ production,
- Large enhancements in charmed meson production in ranges accessible to LHCb.

D^0, D^+, D_s^+, AND D^{*+} CROSS-SECTIONS

5 TeV: JHEP 1706 (2017) 147, 13 TeV: JHEP 1603 (2016) 159 ibid. 1609 (2016) 013, ibid. 1705 (2017) 074

D meson cross-sections now measured at three *pp* collision energies

- $\sqrt{s} = 7\,\mathrm{TeV}$: $\mathcal{L}_{\rm int} = 15\,\mathrm{nb}^{-1}$
  Nucl.Phys. B871 (2013) 1-20,
- $\sqrt{s} = 13\,\mathrm{TeV}$: $\mathcal{L}_{\rm int} = 5\,\mathrm{pb}^{-1}$
  JHEP 1603 159, JHEP 1609 013,
- $\sqrt{s} = 5\,\mathrm{TeV}$: $\mathcal{L}_{\rm int} = 9\,\mathrm{pb}^{-1}$
  arXiv:1610.02230 [hep-ex], submitted to JHEP.

13 TeV and 5 TeV: Analysis of trigger candidates with Turbo† stream.

† Comput. Phys. Commun. 208, 35-42

Separation of prompt and secondary charm with $\log(IP\chi^2)$ distribution.

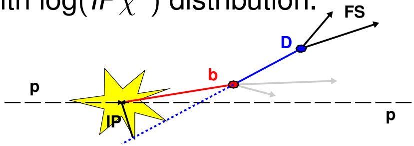

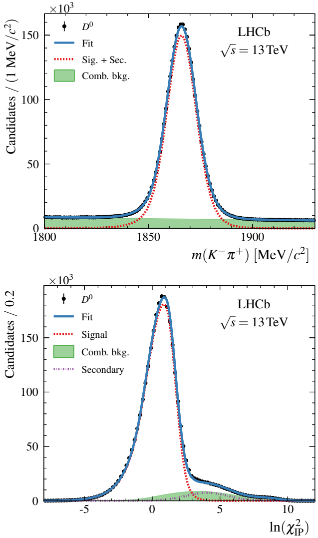

D^0 production at $\sqrt{s} = 13$ TeV (JHEP 1603 (2016) 159)

PROMPT D^0 CROSS-SECTIONS AT $\sqrt{s} = 13\,\text{TeV}$

JHEP 1603 (2016) 159 ibid. 1609 (2016) 013, ibid. 1705 (2017) 074

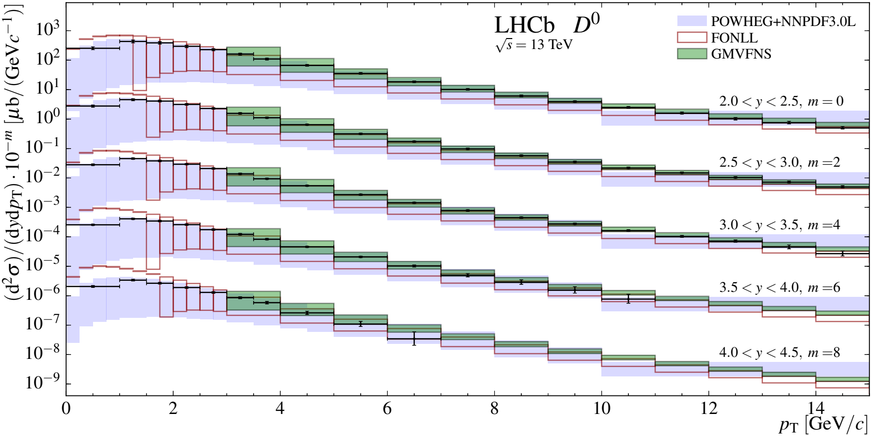

FONLL: Cacciari *et al.*, Eur.Phys.J. C75 (2015) 610,
POWHEG+NNPDF3.0L: Gauld *et al.*, JHEP 1511 (2015) 009,
GMVFNS: Kniehl *et al.*, Eur.Phys.J. C72 (2012) 2082.

Double differential cross-sections, $d^2\sigma_i/dp_T dy$, of prompt D^0 vs. p_T.

Integrated over the acceptance of the analysis

$$\sigma(D^0, p_T < 8\,\text{GeV}, 2.0 < y < 4.5) = 3240 \pm 4 \pm 190\,\mu\text{b}.$$

PROMPT D^0 CROSS-SECTIONS AT $\sqrt{s} = 5\,\text{TeV}$

JHEP 1706 (2017) 147

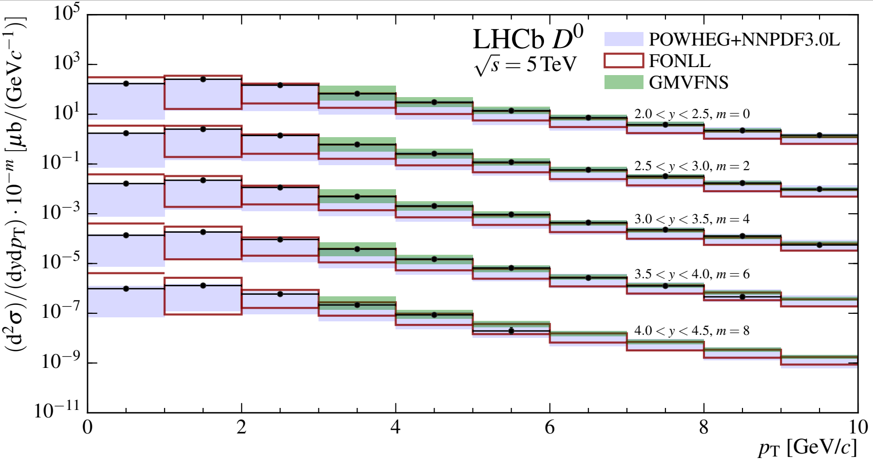

POWHEG+NNPDF3.0L: Gauld *et al.*, JHEP 1511 (2015) 009,
GMVFNS: Kniehl *et al.*, Eur.Phys.J. C72 (2012) 2082.

Double differential cross-sections, $d^2\sigma_i/dp_T dy$, of prompt D^0 vs. p_T.

Integrated over the acceptance of the analysis

$$\sigma(D^0, p_T < 8\,\text{GeV}, 2.0 < y < 4.5) = 1635 \pm 4 \pm 89\,\mu\text{b}.$$

COMPARISONS: 13 TeV RELATIVE TO 7 TeV AND 5 TeV

5 TeV: JHEP 1706 (2017) 147, 13 TeV: JHEP 1603 (2016) 159 ibid. 1609 (2016) 013, ibid. 1705 (2017) 074

13 TeV/ 7 TeV
JHEP 1603 159, JHEP 1609 013, JHEP 1705 074

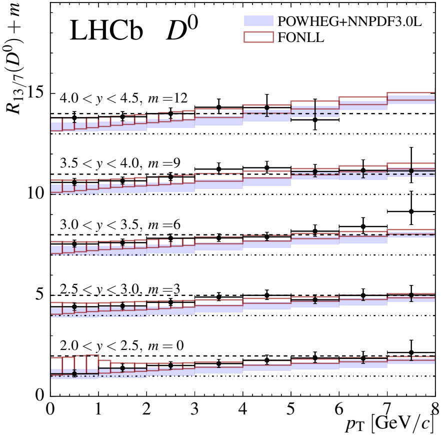

13 TeV/ 5 TeV
JHEP 1706 (2017) 147

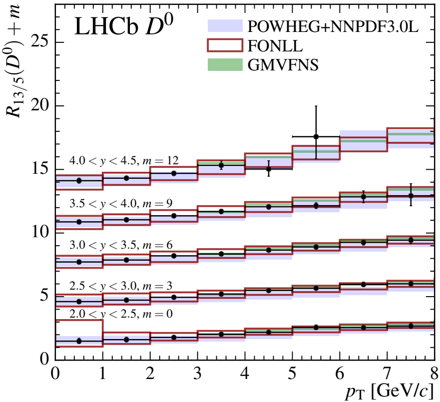

FONLL: Cacciari *et al.*, Eur.Phys.J. C75 (2015) 610,
POWHEG+NNPDF3.0L: Gauld *et al.*, JHEP 1511 (2015) 009,

Ratios of double differential cross-sections, $\mathrm{d}^2\sigma_i/\mathrm{d}p_T\mathrm{d}y$.

For each interval, the dash-dotted line represents a ratio of 1.

RATIOS AT 13 TeV: D^+/D^0

JHEP 1603 (2016) 159 ibid. 1609 (2016) 013, ibid. 1705 (2017) 074

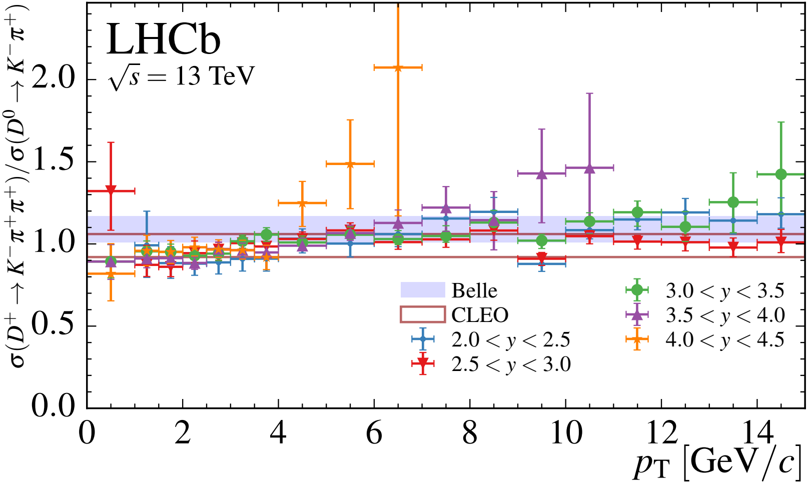

Ratios of double differential cross-sections, $d^2\sigma_i/dp_T dy$, between D^+ and D^0 measurements at $\sqrt{s} = 13$ TeV.

RATIOS AT 5 TeV: D^+/D^0

JHEP 1706 (2017) 147

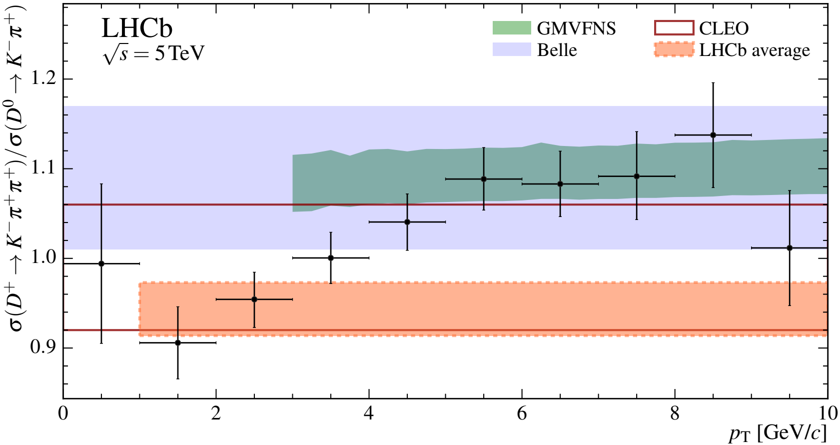

Ratios of differential cross-sections, $\mathrm{d}\sigma_i/\mathrm{d}p_\mathrm{T}$ integrated over $2 < y < 4.5$, between D^+ and D^0 measurements at $\sqrt{s} = 5\,\text{TeV}$.

Multiple heavy quark production

Single Parton Scattering (SPS)

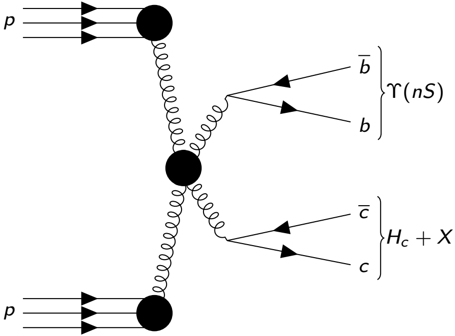

Both heavy flavor pairs from a single hard parton-parton interaction.

NRQCD: (Berezhnoy and Likhoded, IJMPA 30 1550125)

$$R_{\text{SPS}} \equiv \frac{\sigma^{\Upsilon c\bar{c}}}{\sigma^{\Upsilon}} = (0.2 - -0.6)\%.$$

Double Parton Scattering (DPS)

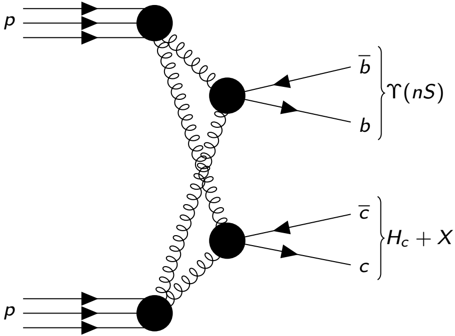

Two independent parton collisions.

$$\sigma^{\Upsilon c\bar{c}} = \frac{\sigma^{\Upsilon} \times \sigma^{c\bar{c}}}{\sigma_{\text{eff}}}$$

$$R_{\text{DPS}} \equiv \frac{\sigma^{\Upsilon c\bar{c}}}{\sigma^{\Upsilon}} = \frac{\sigma^{c\bar{c}}}{\sigma_{\text{eff}}} \approx 10\%.$$

$\Upsilon + D$ ASSOCIATED PRODUCTION

JHEP 1607 (2016) 052

LHCb Run 1 data

- $1\,\text{fb}^{-1}$ of pp at $\sqrt{s} = 7\,\text{TeV}$,
- $2\,\text{fb}^{-1}$ of pp at $\sqrt{s} = 8\,\text{TeV}$.

Coincidences of $b\bar{b}$ states and open charm,

- $\Upsilon(n\text{S}) \to \mu^+\mu^-$ for $n = 1, 2, 3$,
- D^0, D^+, D_s^+, and Λ_c^+ in decays to CF hadronic modes.

First observations in excess of $5\,\sigma$ significance for 5 combinations,
$\Upsilon(1\text{S})$+D^0, $\Upsilon(1\text{S})$+D^+, $\Upsilon(1\text{S})$+D_s^+, $\Upsilon(2\text{S})$+D^0, and $\Upsilon(2\text{S})$+D^+.

Measured cross-sections and differential distributions of kinematic variables.

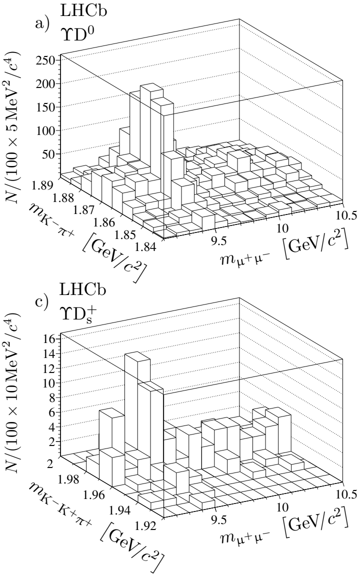

$\Upsilon + D$ VIA DPS

JHEP 1607 (2016) 052

Measured cross-sections

$$\sigma^{\Upsilon(1S)D^0}_{\sqrt{s}=7\,\text{TeV}} \times \mathcal{B}(\Upsilon(1S) \to \mu^+\mu^-) = 155 \pm 21 \pm 7\,\text{pb},$$
$$\sigma^{\Upsilon(1S)D^+}_{\sqrt{s}=7\,\text{TeV}} \times \mathcal{B}(\Upsilon(1S) \to \mu^+\mu^-) = 82 \pm 19 \pm 5\,\text{pb}.$$

From which are computed

$$R_{\sqrt{s}=7\,\text{TeV}} \left.\frac{\sigma^{\Upsilon(1S)c\bar{c}}}{\sigma^{\Upsilon(1S)}}\right|_{\sqrt{s}=7\,\text{TeV}} = (7.7 \pm 1.0)\%.$$

Significantly larger than theoretical predictions.

Azimuthal angle, $\Delta\phi$, between Υ and D

- Flat, consistent with independent,
- Production dominated by DPS.

Computations of normalization factor σ_{eff} assuming DPS,

$$\sigma_{\text{eff}}\big|_{\Upsilon(1S)D^0} = 19.4 \pm 2.6 \pm 1.3\,\text{mb}$$

consistent with values from previous measurements in other channels

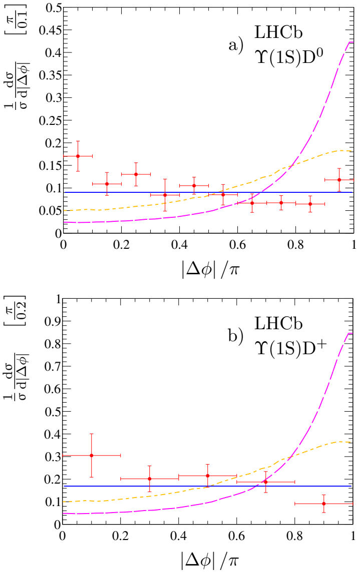

UNIVERSALITY OF σ_{eff}

JHEP 1607 (2016) 052

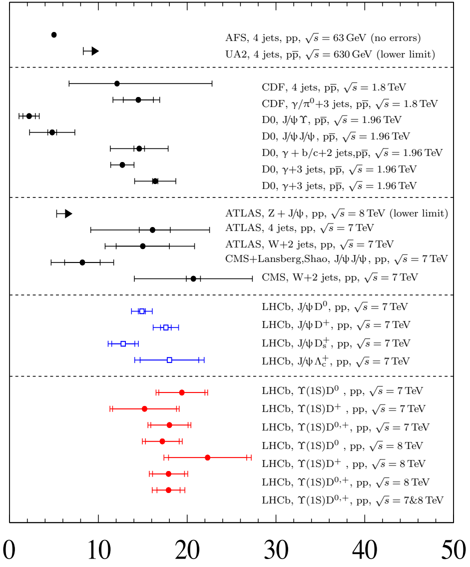

MASS FITS FOR $D^{*+}\pi^-$

JHEP 1309 145

Enhanced unnatural parity

$|\cos\theta_{\mathrm{H}}| > 0.75$

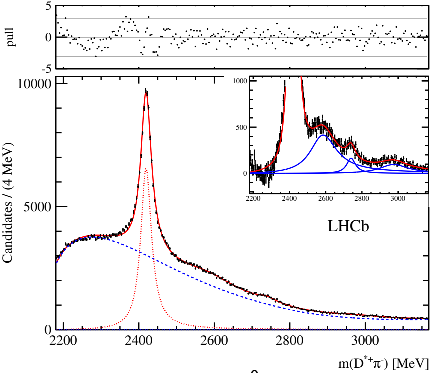

Dominated by $D_1(2420)^0$.

Three additional structures observed $D_J(2580)^0$, $D_J(2740)^0$, $D_J(3000)^0$.

Natural parity subsample

$|\cos\theta_{\mathrm{H}}| < 0.5$

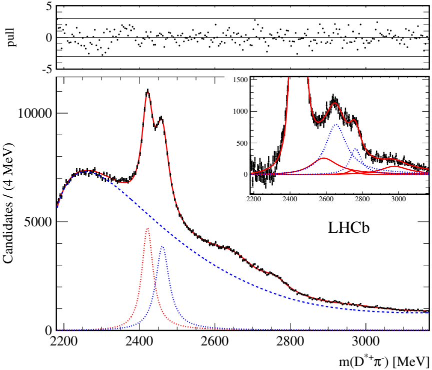

Large $D_1(2420)^0$ and $D_2^*(2460)^0$ features.

$D_J(2580)^0$, $D_J(2740)^0$, and $D_J(3000)^0$, fixed

Two additional structures observed

$D_J^*(2650)^0$, $D_J^*(2760)^0$

ANGULAR ANALYSIS OF $D^{*+}\pi^-$

JHEP 1309 145

Data set partitioned in to 10 slices of helicity angle.

Yields of each structure determined as a function of $\cos\theta_{\mathrm{H}}$.

$D_1(2420)^0$ and $D_2^*(2460)^0$ consistent with expected $J^P = 1^+$ and 2^+ respectively.

$D_J^*(2650)^0$ and $D_J^*(2760)^0$ consistent with having natural parity.

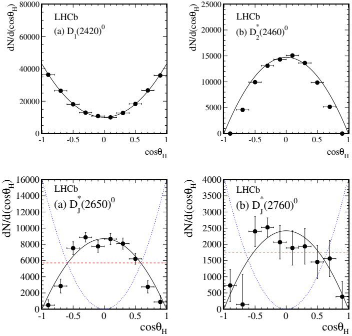

Angular distributions for $D_J(2580)^0$, $D_J(2740)^0$, and $D_J(3000)^0$ are consistent with having unnatural parity.

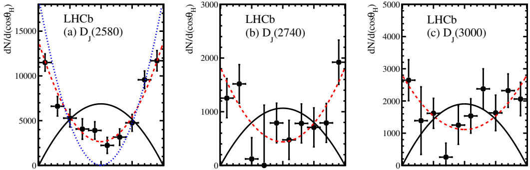

DALITZ ANALYSIS OF $B^- \to D^+\pi^-\pi^-$

Phys. Rev. D 94, 072001 (2016)

Dalitz analysis of $27\,956 \pm 195$ $B^- \to D^+\pi^-\pi^-$ decays

- Signal purity $\sim$98.5%

Full 3 fb^{-1} of LHCb Run 1 data.

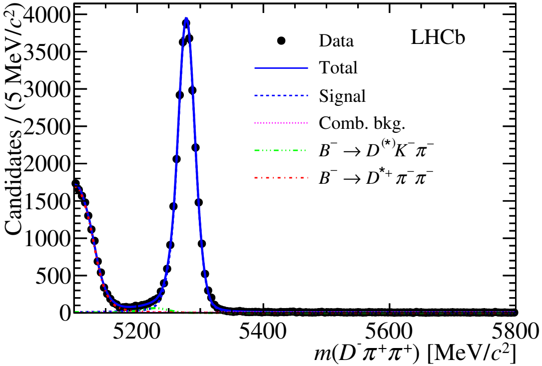

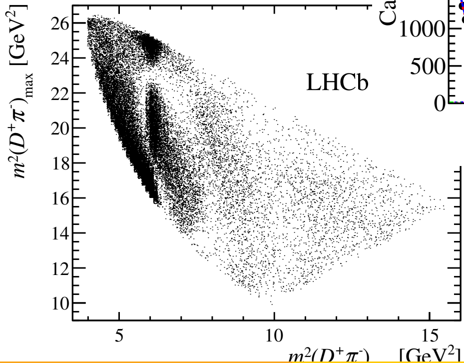

Identical pions ordered by magnitude of $m^2(D^+\pi^-)$
$m^2(D^+\pi^-)_{\text{min}}$, $m^2(D^+\pi^-)_{\text{max}}$

DALITZ ANALYSIS OF $B^- \to D^+\pi^-\pi^-$

Phys. Rev. D 94, 072001 (2016)

Resonance	Fit fraction (%)
$D_2^*(2460)^0$	$35.69 \pm 0.62 \pm 1.37 \pm 0.89$
$D_1^*(2680)^0$	$8.32 \pm 0.62 \pm 0.69 \pm 1.79$
$D_3^*(2760)^0$	$1.01 \pm 0.13 \pm 0.13 \pm 0.25$
$D_2^*(3000)^0$	$0.23 \pm 0.07 \pm 0.07 \pm 0.08$
$D_v^*(2007)^0$	$10.79 \pm 0.68 \pm 0.74 \pm 2.34$
B_v^*	$2.69 \pm 1.01 \pm 1.43 \pm 1.61$
Total S-wave	$56.96 \pm 0.78 \pm 0.62 \pm 0.87$

Resonance parameters (MeV)	
$D_2^*(2460)^0$	$m = 2463.7 \pm 0.4 \pm 0.4 \pm 0.6$
	$\Gamma = 47.0 \pm 0.8 \pm 0.9 \pm 0.3$
$D_1^*(2680)^0$	$m = 2681.1 \pm 5.6 \pm 4.9 \pm 13.1$
	$\Gamma = 186.7 \pm 8.5 \pm 8.6 \pm 8.2$
$D_3^*(2760)^0$	$m = 2775.5 \pm 4.5 \pm 4.5 \pm 4.7$
	$\Gamma = 95.3 \pm 9.6 \pm 7.9 \pm 33.1$
$D_2^*(3000)^0$	$m = 3214 \pm 29 \pm 33 \pm 36$
	$\Gamma = 186 \pm 38 \pm 34 \pm 63$

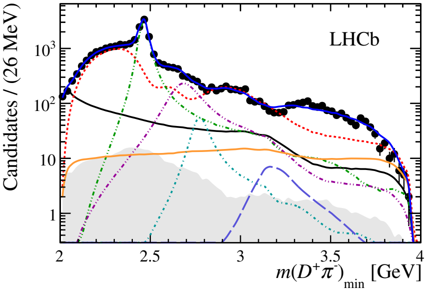

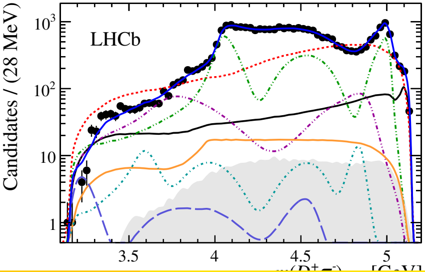

First observations of $D_3^*(2760)^0$, $D_2^*(3000)^0$

- Parameters of $D_3^*(2760)^0$ with $D_J^*(2760)$

DOUBLY CHARMED BARYONS AT OTHER EXPERIMENTS

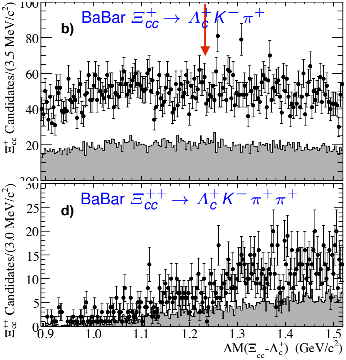

BaBar: Phys.Rev. D74 (2006) 011103

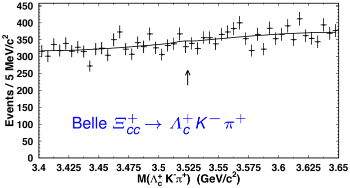

Belle: Phys.Rev.Lett. 97 (2006) 162001

FOCUS: Photon beam on Be fixed target

Nucl.Phys.Proc.Suppl. 115 (2003) 33-36

- Search for both Ξ_{cc}^{+} and Ξ_{cc}^{++},
- 7 exclusive $\Xi_{cc} \to \Lambda_c^+ X$ modes,
- 14 exclusive $\Xi_{cc} \to D^{0,+} Y$ modes,
- No evidence of Ξ_{cc}.

BaBar: e^+e^- at $\Upsilon(4S)$ Phys.Rev. D74 (2006) 011103

- Search for both Ξ_{cc}^{+} and Ξ_{cc}^{++},
- $\Xi_{cc}{}^{+(+)} \to \Lambda_c^+ K^- \pi^+ (\pi^+)$
- $\Xi_{cc}{}^{+(+)} \to \Xi_c^0 \pi^+ (\pi^+)$
- No evidence of Ξ_{cc}.

Belle: e^+e^- at $\Upsilon(4S)$ Phys.Rev.Lett. 97 (2006) 162001

- Searched for $\Xi_{cc}^{+} \to \Lambda_c^+ K^- \pi^+$,
- Found new Ξ_c^+ resonance decaying to $\Lambda_c^+ K^- \pi^+$
- No evidence of Ξ_{cc}.

LHCb's first search for Ξ_{cc}^{+}

JHEP 1312 (2013) 090

Initial search at LHCb in $\Xi_{cc}^{+} \to \Lambda_c^{+} K^{-} \pi^{+}$:

- The initial SELEX mode with a large expected BF.
- Based on $0.65\,\text{fb}^{-1}$ of 2011 data.

No evidence of Ξ_{cc}^{+} production.

- Set upper limits on production
  $R \equiv \frac{\sigma(\Xi_{cc}^{+})\mathcal{B}(\Xi_{cc}^{+} \to \Lambda_c^{+} K^{-} \pi^{+})}{\sigma(\Lambda_c^{+})}$
  as function of mass and lifetime,

  $R < 0.013$ for $\tau = 100\,\text{fs}$

  $R < 3.3 \times 10^{-4}$ for $\tau = 400\,\text{fs}$
- Due limited sensitivity at short lifetimes, this non-observation is not inconsistent with the SELEX claim.

$\delta m \equiv m(\Lambda_c^{+} K \pi) - m(\Lambda_c^{+}) - m(K) - m(\pi)$

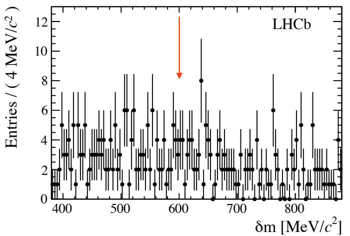

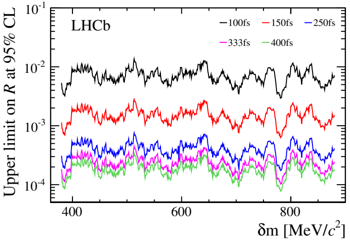

Charm production at $\sqrt{s} = 13\,\text{TeV}$

LHCb has some of the world's largest charm data sets,
$$\sigma(pp \to c\bar{c}X;\, 13\,\text{TeV})_{\text{LHCb}} = 2369 \pm 3 \pm 192\,\mu\text{b}$$

JHEP 1603 (2016) 159, erratum JHEP 1705 (2017) 074

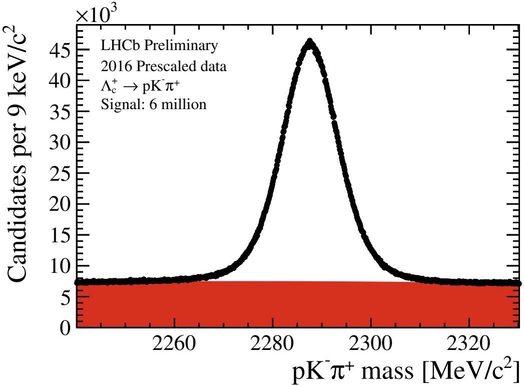

$\sim$10% of 2016 data.

Large, high-purity samples of $\Lambda_c^+ \to pK^-\pi^+$

- 2016 search dataset: $\int \mathcal{L} = 1.7\,\text{fb}^{-1} \Rightarrow \sim$60 million $\Lambda_c^+ \to pK^-\pi^+$.

Confirmation in Run 1 dataset

arXiv:1707.01621, accepted by Phys.Rev.Lett.

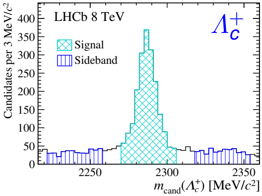

Similar search in Run 1 data collected in 2012,

- $\int \mathcal{L} = 2\,\text{fb}^{-1}$ in pp collisions at 8 TeV,
- Different trigger and data processing configuration.

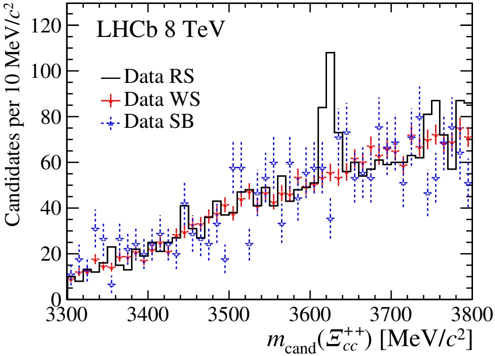

Again, clear structure visible,

- Yield: 113 ± 21 decays,
- Local significance: $> 7\sigma$ (likelihood ratio).

Fitted mass consistent with structure in Run 2 data:

$$m(\Xi_{cc}^{++})_{\rm R1} - m(\Xi_{cc}^{++})_{\rm R2} = 0.8 \pm 1.4\,\text{MeV}.$$

(statistical uncertainty only)

SELEX AND Ξ_{cc}^{++}

NEVER PUBLISHED

In unpublished work that was shown at several conferences, the SELEX collaboration did claim to have seen two *ccu* states in the $\Lambda_c^+ K^- \pi^+ \pi^+$ mass spectrum.

$\Xi_{cc}(3780)^{++}$:

- Width greater than detector resolution,
- Contained $\Lambda_c^+ K^- \pi^+$ combinations from the Ξ_{cc}^+ observation,
- Interpreted as an excited state.

$\Xi_{cc}(3452)^{++}$:

- Also claimed evidence in $\Xi_c^+ \pi^+ \pi^- \pi^+$,
- $67 \pm 3\,\mathrm{MeV}$ below their Ξ_{cc}^+ mass.

See the talks and proceedings linked from the SELEX web pages.

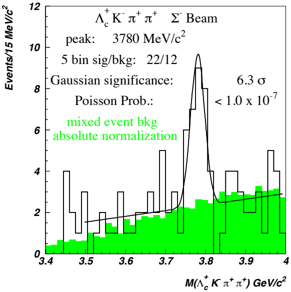

J. Engelfried for the SELEX collaboration, proceedings of HQL06, hep-ex/0702001.

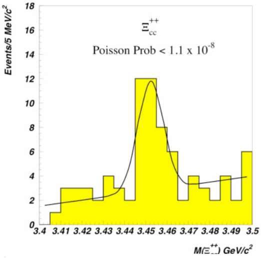

P. Cooper, slides in proceedings of Charm2007.